



**HAL**  
open science

## Thermal characterization of a biodiesel nitration: Bio-additive's synthesis by calorimetric methods

Adji Diop, Imed Ben Talouba, Laurent Balland, Nordine Mouhab

### ► To cite this version:

Adji Diop, Imed Ben Talouba, Laurent Balland, Nordine Mouhab. Thermal characterization of a biodiesel nitration: Bio-additive's synthesis by calorimetric methods. *Thermochimica Acta*, 2019, 673, pp.138-146. 10.1016/j.tca.2019.01.024 . hal-02138408

HAL Id: hal-02138408

<https://hal.science/hal-02138408v1>

Submitted on 21 Oct 2021

**HAL** is a multi-disciplinary open access archive for the deposit and dissemination of scientific research documents, whether they are published or not. The documents may come from teaching and research institutions in France or abroad, or from public or private research centers.

L'archive ouverte pluridisciplinaire **HAL**, est destinée au dépôt et à la diffusion de documents scientifiques de niveau recherche, publiés ou non, émanant des établissements d'enseignement et de recherche français ou étrangers, des laboratoires publics ou privés.



Distributed under a Creative Commons Attribution - NonCommercial 4.0 International License

# 1 Thermal characterization of a biodiesel nitration: 2 bio-additive's synthesis by calorimetric methods

3 DIOP Adj, BEN TALOUBA Imed <sup>\*1</sup>, BALLAND Laurent, MOUHAB Nordine

4 Laboratoire de Sécurité des Procédés Chimiques (LSPC-EA4704), Normandie Univ, UNIROUEN, 76000  
5 Rouen, France

## 6 Abstract

7 The aim of this study was to synthesize a substitute to the 2-Ethyl Hexyl Nitrate (EHN) by  
8 nitrating a biodiesel. EHN is commonly used to improve the auto-ignition properties of diesel  
9 fuels. The biodiesel was obtained by trans-esterification of canola oil. The nitration reaction  
10 was carried out in a reaction calorimetry RC1 with semi-batch mode to study its exothermic  
11 behavior. Mixed sulfuric/nitric acid was used as nitrating agent. The impact of the synthesis  
12 temperature on the thermal behavior and on the reaction medium composition was  
13 investigated. The final product was analyzed by using several analytical techniques such as  
14 iodine number, infrared spectrometry, GC-MS and mass spectrometry. This analytical study  
15 combined with the results of thermal stability study in DSC, allowed to highlight that  
16 chemical transformations play an important role on the thermal reaction behavior and on the  
17 Maximum Temperature of the Synthesis Reaction (*MTSR*). In addition to the mixed acid  
18 decomposition, the synthesis at high temperature involves the production of nitrated products:  
19 methyl-8-nitro oleate, methyl-10-nitrate stearate, methyl-10-nitrate-9-nitrostearate. Also, the  
20 Cooperative Fuel Research (CFR) engine was used to analyze the cetane number of diesel  
21 fuel mixed with our additive according to the ASTM D613 standard. The results showed an  
22 increase in cetane number of 3.2 points.

23  
24 Keywords: methyl oleate, cetane number, reaction calorimeter, DSC, *MTSR*

## 25 1 Introduction

26 The industrialization and motorization in recent years come along with a high demand for  
27 petroleum products and an increase in air pollution [1]. It has been established by the  
28 Interprofessional Center for Technical Studies of Atmospheric Pollution (CITEPA), in  
29 France, that the automotive sector (mainly diesel engines) plays a leading role in air pollution  
30 ( $\text{CO}_2$ , CO,  $\text{NO}_x$ ,  $\text{SO}_2$ ).

31 To reduce the pollution related to diesel engines, several solutions have been tested including  
32 the setting up of catalytic oxidation pots, particles filters [2] and the use of additives, mainly  
33 cetane number improvers [3].

34 Cetane improver additives are commonly used to increase engine performances. According to  
35 Beatrice *et al* 1996 [4], an increase in the cetane number reduces  $\text{NO}_x$  and particle emissions.  
36 There are a lot of cetane number improvers [5] [6] but the 2-EthylHexyl Nitrate (ENH) is the  
37 main additive used for diesel. The EHN is an energy molecule obtained by nitration of iso-  
38 octanol (fossil fuels) with mixed nitric/sulfuric acid (1:1.5 w/w).

---

\*imed.bentalouba@univ-rouen.fr

39 Several studies showed that the iso-octanol nitration is a strongly exothermic reaction which  
40 takes place in a heterogeneous liquid-liquid mixture [7] [8]. EHN additive is thermally  
41 unstable and sensitive to heat. Its thermal instability is mainly due to energetic functional  
42 groups like nitro (C–NO<sub>2</sub>) and nitrate (C–O–NO<sub>2</sub>). Those functional groups are composed of  
43 easily broken C–N covalent bonds. In fact, according to Yang et al 2014 [9], several  
44 industrial accidents in China are due to the loss of control during the EHN synthesis. The  
45 thermal behavior of this reaction need to be carefully investigated to assess the associated  
46 risks [10].

47 With the scarcity of fossil fuels, it is important to reduce the dependency on petroleum  
48 products. The goal of the work described in this article is to synthesize a substitute to the  
49 EHN by nitrating a trans-esterified vegetable oil (biodiesel). Many studies on the use of  
50 biodiesel as biofuels [11][12] or as bio-additive [13] have been realized over the years. The  
51 biodiesel's particularity is that it contains less carbon, less sulfide, less water and more  
52 oxygen atoms than fossil diesel. Therefore, it is less dangerous for humans [14] and its  
53 amount of oxygen atoms improves combustion [15].

54 In this article, the biodiesel obtained from canola oil was used. According to Abdullah et al  
55 2010 [16], the presence of double bonds favors the nitration reaction. And the canola oil has a  
56 lot of double bounds compared to the other vegetable oils. The classic mixed sulfuric/nitric  
57 acid [17] (1.5:1 w/w) was used as the nitrating agent.

58 First, a study about the identification and the characterization of the chemical compounds that  
59 results from nitration by various analytical techniques (infrared spectrometer, GCMS, electro  
60 spray ionization mass spectrometer, and iodine index measurement) was conducted. Then, a  
61 complete study on the thermal stability of the reaction mixture (reagents and products) was  
62 realized. This study uses the thermal information given by a reaction calorimeter RC1 and a  
63 DSC type microcalorimeter. The quality of the synthesized bio-additive was determined by  
64 measuring its cetane number according to the ASTM standard D 613.

## 65 **2 Materials and products**

### 66 **2.1 Products**

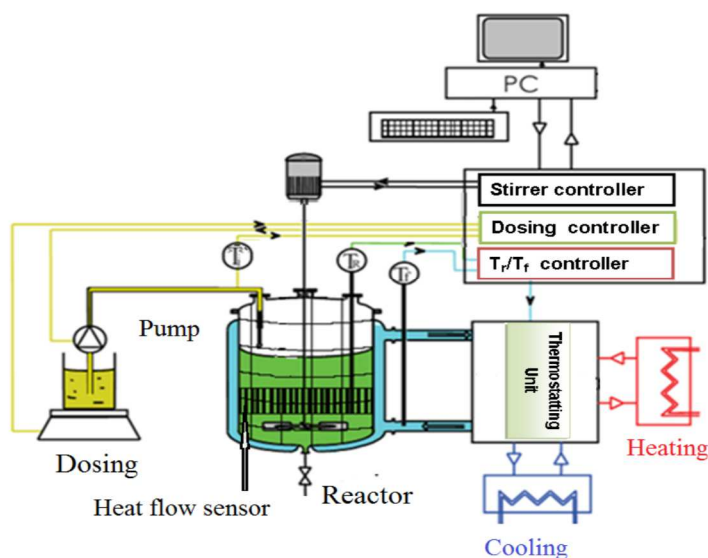
67 The biodiesel (Diester®) used was obtained by trans-esterification of canola oil and was  
68 provided by Saipol company (Grand-Quevilly-France). Nitric (65%w/w), sulfuric (95% w/w)  
69 acids used as nitrating agent and solvents (potassium iodide 1% volumetric, sodium  
70 thiosulfate (Na<sub>2</sub>S<sub>2</sub>O<sub>3</sub>) 0.1M, bicarbonate solution for analysis (>99.7%) and Wijs reactive 0.1  
71 mol·L<sup>-1</sup>) are provided by Fisher Chemical. The methyl nonadecanoate (> 98%) for GC  
72 analysis was supplied by Sigma Aldrich.

### 73 **2.2 Materials**

- 74     ▪ Calorimetric reactor RC1-RTCal

75 The nitration was carried out in a calorimetric reactor RC1-RTCal (Mettler®) operating in  
76 semi-batch mode. It is equipped with an AP00-0.5-RTCal reactor vessel with 0.5L capacity.  
77 Mixing system is made of an impeller with one baffle. The experimental device is presented

78 in Fig. 1. The reactor has a temperature control system (between  $-20^{\circ}\text{C}$  and  $+165^{\circ}\text{C}$ ) and an  
79 *RTCal* measurement technology based on thermal flow sensors located on the reactor wall.  
80 The temperature regulation includes a thermostatic group which takes care of the various  
81 regulation modes thanks to a fluid (Rodorsil 47 V20). This device provides real-time  
82 monitoring of the heat released by the nitration reaction which is highly exothermic.



83

84

Fig. 1. Reaction calorimeter RC1-RTCal (Mettler®)

85

- Differential Scanning Calorimeter DSC Q20

86 The reactive and products stability study was based on thermograms analysis obtained with  
87 the DSC Q20. The DSC was provided by TA Instruments with purge using extra pure  
88 nitrogen ( $50 \text{ mL}\cdot\text{min}^{-1}$ ). It can work in isothermal and non-isothermal conditions. DSC  
89 measures temperature with accuracy of  $\pm 0.05 \text{ K}$ . Its specific sensitivity is  $1\text{mW}\cdot\text{kg}^{-1}$ [18].The  
90 device detects temperature changes between the sample and the reference to measure heat  
91 flow over time and temperature. Gold-plated high pressure crucibles (M20 crucibles from  
92 Swiss Institute for the Promotion of Safety and Security) were used for measurement [19].

93

- Chemical analysis materials

94 The FTIR IR Affinity-1S from Shimadzu ( $400$  to  $4000 \text{ cm}^{-1}$ ), GC-MS from Agilent  
95 technology 7890A GC/5975C VL MSD, and the mass spectrometry with electro spray  
96 ionization from Waters LCT Premier were used to identify and quantify chemical species.

97 GC-MS analyses were performed in a GC6850 gas chromatography coupled with a 5975C  
98 MSD Quad Instrument with electrons impact ionization at  $70 \text{ eV}$ . A HP5-MS 5% Phenyl  
99 Methyl Siloxane capillary column (Agilent 19091S-433E) with a  $0.25 \text{ mm}$  i.d.,  $30 \text{ m}$  nominal  
100 length and  $0.25 \mu\text{m}$  phase film diameter was used. The carrier gas was helium at a flow rate of  
101  $15 \text{ mL}\cdot\text{min}^{-1}$ .

## 102 3 Synthesis and chemical analysis

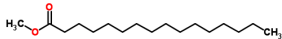
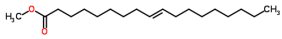
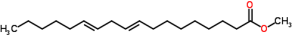
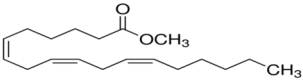
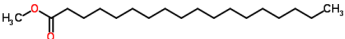
### 103 3.1 Experiment

104 Considering the chemical instability of the mixed acid (nitrating agent), it was prepared just  
105 before the synthesis reaction (nitration). 86.4 g of sulfuric acid was introduced with a flow  
106 rate of  $4\text{g}\cdot\text{min}^{-1}$  into the reaction calorimeter filled with 57.6 g of nitric acid. The mixture was  
107 stirred at 200 rpm and kept at  $5^\circ\text{C}$  during the addition. At the end, the mixture, composed of  
108  $\text{HNO}_3$  27 %,  $\text{H}_2\text{SO}_4$  58%,  $\text{H}_2\text{O}$  15% (w/w), was kept in the fridge at the same temperature.

109 To carry out the synthesis reaction, 144g of mixed acid was dosed with a flow rate of  $4\text{g}\cdot\text{min}^{-1}$   
110 into the reactor initially filled with 150 g of biodiesel composed of 92% of methyl oleate  
111 (determined by GC-MS Table 1). These operating conditions are chosen after preliminary  
112 study on the effect of parameters such as a flow rate, stirring speed on thermal behavior in  
113 order to ensure the safe operation of the reactor. The synthesis reaction was carried out at 600  
114 rpm stirring speed, in the isothermal mode. This experiment was realized at seven different  
115 temperatures (10-15-20-25-30-40 and  $50^\circ\text{C}$ ). The Mettler RC1 operating software allows to  
116 record the thermal signal (power profile) and to monitor the reaction progress. The final  
117 product was then transferred to a separating funnel and separated in two phases. Only the  
118 organic phase (which contains the nitrated products) was analyzed. Before the analysis, the  
119 organic phase was, first, washed with a bicarbonate solution at 2% w/w, and then with  
120 distilled water until a neutral pH was obtained.

121

Table 1: Fatty Acid Methyl Esters (FAME) from canola composition

Compounds	% w/w
Methyl palmitate	
	2.2
Methyl oleate	
	92.0
Methyl linoleate	
	2.5
Methyl linolenate	
	2.8
Methyl stearate	
	0.5

122

123 **3.2 Nitration Product analysis**

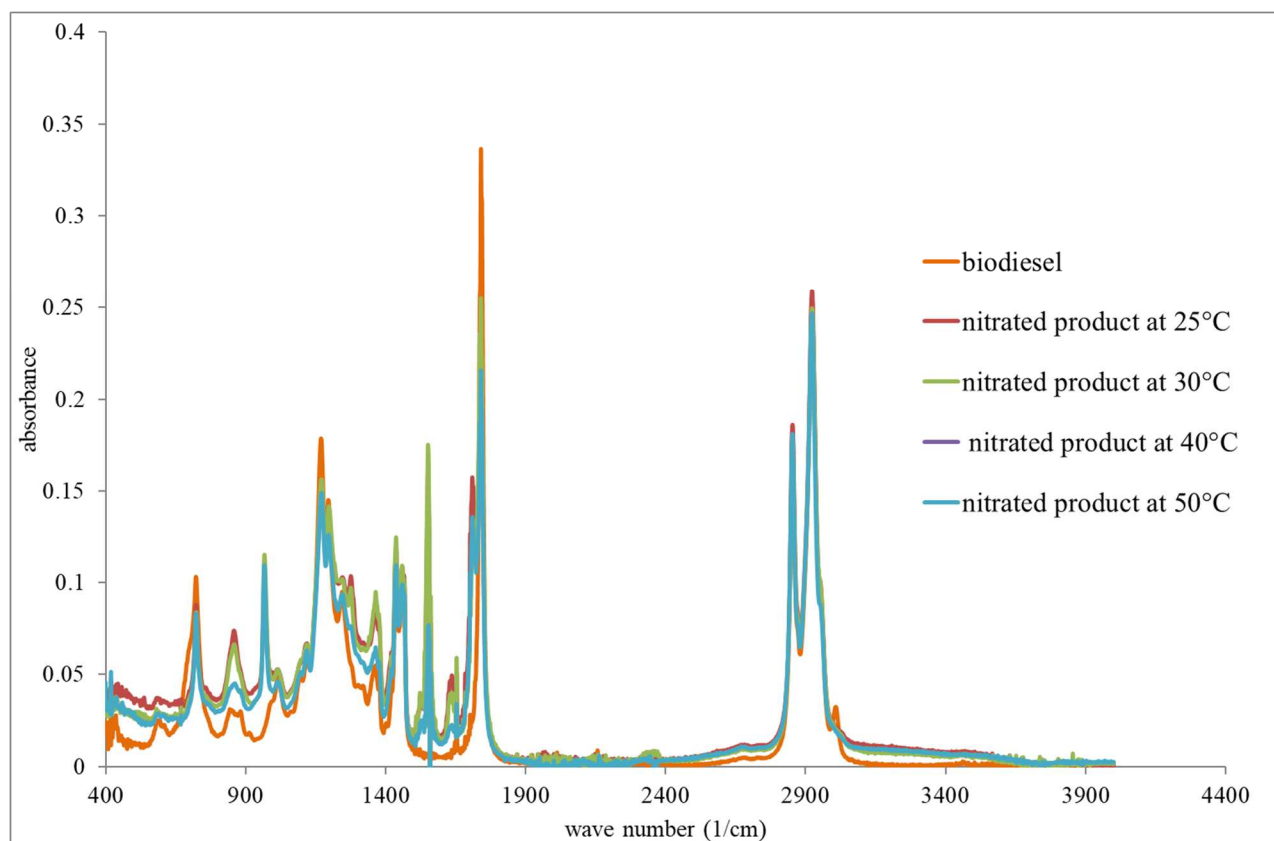
124 Infrared analysis and electro-spray ionization mass spectrometry were used to identify and  
125 quantify the different chemical compounds produced during the biodiesel nitration.

126 **3.2.1 Infrared analysis**

127 Fig. 2 shows the FTIR spectra of biodiesel and nitrated products at different temperatures.  
128 These spectra were obtained after defining the baseline corresponding to the air spectrum with  
129 50 scans. An absorbance difference is noted between 800 and 1700  $\text{cm}^{-1}$ . It allows to identify  
130 new functional groups present in the nitrated product (Table 2). The value of the nitrated  
131 products absorbance depends on the synthesis temperature.

132 The characteristic ester frequency C=O bonds at 1750  $\text{cm}^{-1}$ , alkane frequency C-H bonds  
133 between 2900-3000  $\text{cm}^{-1}$  and alkene frequency C=C stretch at 1650  $\text{cm}^{-1}$  with weak intensity,  
134 obviously appear in all spectra. The spectrum of the nitrated product shows the presence of  
135 three new peaks at 1363, 1550 and at 1635  $\text{cm}^{-1}$ . They respectively indicate the stretching of  
136 symmetric  $\text{NO}_2$ , that of assymmetric  $\text{NO}_2$  and the absorption of  $\text{ONO}_2$  (fig.3).

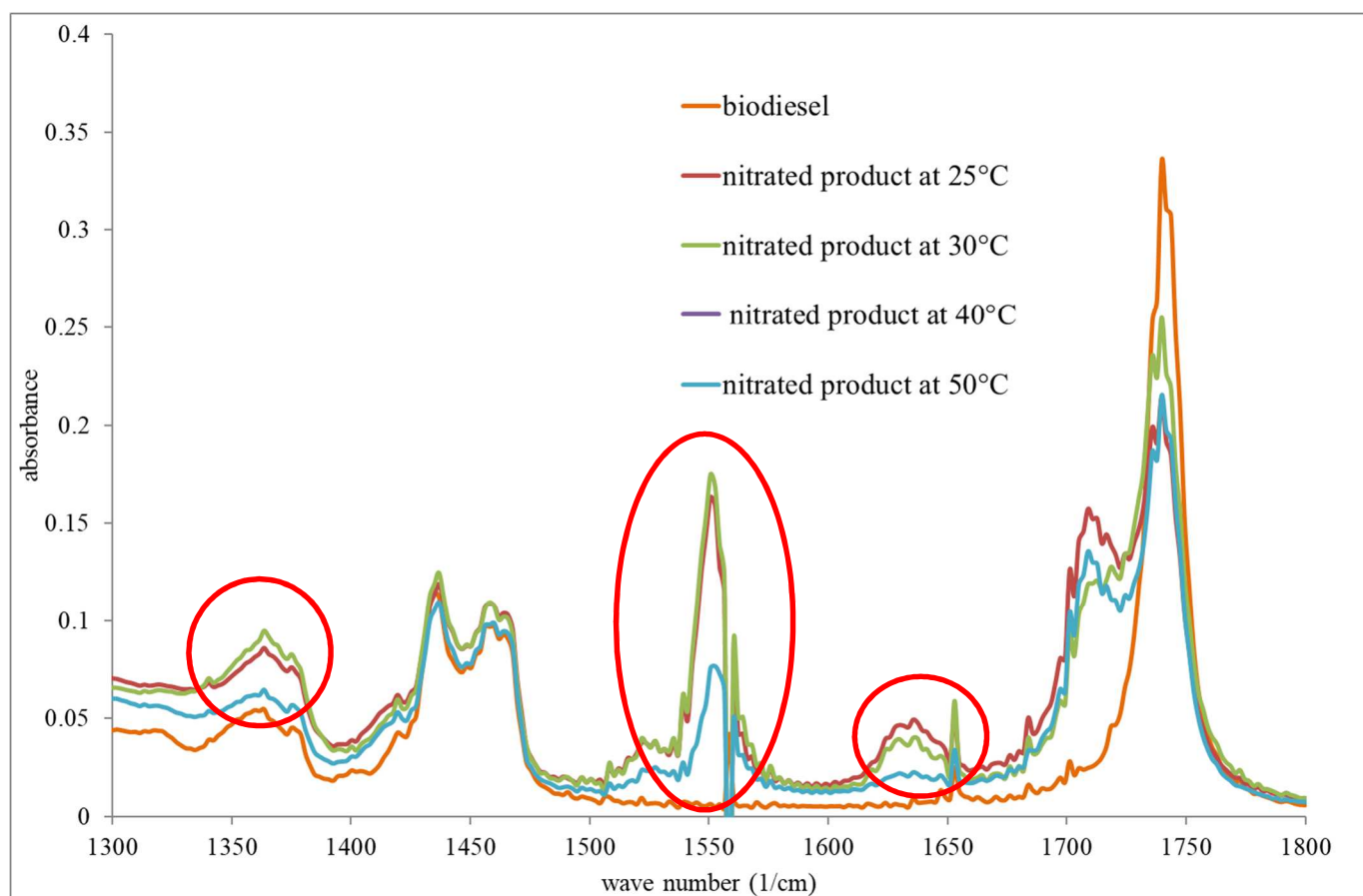
137 The absorption spectrum at 1363 $\text{cm}^{-1}$  (fig.3) indicating a symmetric vibration of R- $\text{NO}_2$  for  
138 nitrated products, can also be observed in biodiesel but is less intense. This peak in the  
139 biodiesel spectrum corresponds to the vibration of  $\text{CH}_2$  groups which is supposed to appear at  
140 1370  $\text{cm}^{-1}$ .



141

142

Fig. 2. IR spectra of biodiesel and nitrated products at different temperatures



143

144

Fig. 3. Zoom on the IR spectra

145

Table 2: Determination of new functional groups after the reaction

Groups	Theoretical wave number $\text{cm}^{-1}$	Experimental wave number $\text{cm}^{-1}$
RNO <sub>2</sub> (Asymmetric)	1560-1548	1550
RNO <sub>2</sub> (Symmetric)	1397-1310	1363
RONO <sub>2</sub>	1640-1620	1635

146

147 To complete this IR analysis which only identifies the functional groups, electro spray  
 148 ionization mass spectrometry was used to identify the synthesized molecules.

### 149 3.2.2 Electro spray ionization mass spectrometry

150 The electro spray ionization mass spectrometry allows to avoid the degradation of the nitrated  
 151 products during the heating in the chromatography column. The samples (biodiesel and nitro  
 152 product) were diluted with acetonitrile to a concentration of 20  $\mu\text{g}/\text{mL}$ , before being  
 153 introduced into a capillary tube with a flow rate of 15  $\mu\text{L}\cdot\text{min}^{-1}$ . Peaks of the spectrum in Fig.  
 154 4a correspond to methyl oleate, methyl linolenate and the methyl linoleate. These molecules  
 155 are in a ionic adduct form  $[\text{M} + \text{Na}]^+$  at  $m/z = 319$ ,  $m/z = 315$  and  $m/z = 317$ .

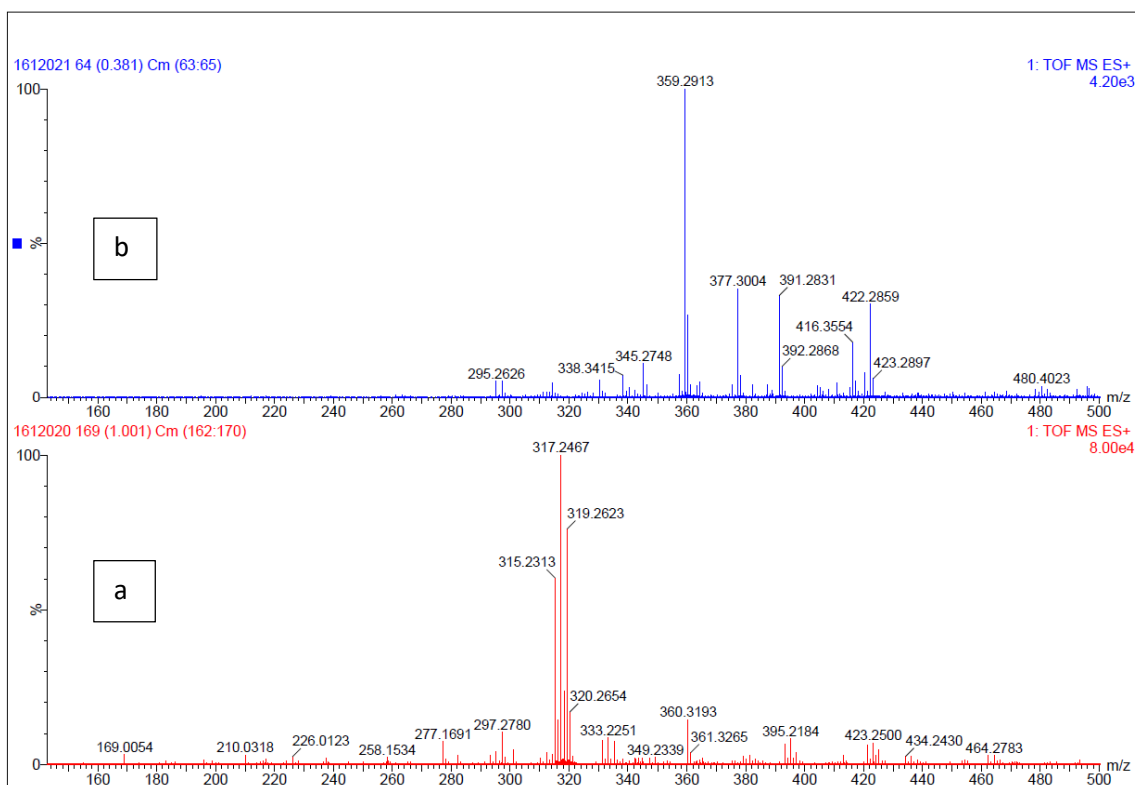


Fig. 4. Biodiesel and nitrated biodiesel mass spectrum

For the nitrated biodiesel (Fig. 4b), intense peaks at  $m/z$  359, 377 and 422 are observed. These peaks correspond to  $[M+NH_4]^+$  ion. Table 3 shows the different identified compounds.

Table 3: Molecules after the nitration reaction

Empirical formula	Molar mass	Structural formula
$C_{19}H_{35}NO_4$ A (Methyl-8-nitro oleate)	$341\text{g}\cdot\text{mol}^{-1}$	
$C_{19}H_{37}NO_5$ B (Methyl-10-nitrate stearate)	$359\text{g}\cdot\text{mol}^{-1}$	
$C_{19}H_{36}N_2O_7$ C (Methyl-10-nitrate-9-nitrostearate)	$404\text{g}\cdot\text{mol}^{-1}$	

156

157

158

159

160

161



162 This study reveals that the nitration reaction can be performed on the carbon atoms carrying  
163 the double bond as well as those in the beta position. This result contradicts Abdullah *et al*  
164 (2010) [16] work which indicates that during the nitration process the NO<sub>2</sub> or NO<sub>3</sub> groups are  
165 attached only on the unsaturated carbon atoms.

166 Three compounds were identified A (Methyl-8-nitro oleate), B (Methyl-10-nitrate  
167 stearate) and C (Methyl-10-nitrate-9-nitrostearate).

### 168 3.3 Study of the reaction selectivity

169 GC-MS and iodine index measurement were used to determine the molar proportion of each  
170 compound A, B and C.

#### 171 3.3.1 Measurement of the conversion rate

172 The nitration reaction's conversion rate was determined by using a GC-MS with addition of  
173 an internal standard (methyl nonadecanoate) according to the 2011 EN14103 standard. Each  
174 solution was dissolved in 10 mL of toluene (GC purity  $\geq 99.5\%$ ). 2 $\mu$ L of the sample was  
175 injected in the column previously heated at 60°C. This column was heated to 200°C with a  
176 10°C/min heating rate then at 5 °C·min<sup>-1</sup> to 240°C. Finally, the column was maintained at this  
177 temperature during 7 min. The runtime was 30 min. Splitless mode was used.

178 Results are presented in Table 4

179 *Table 4: Total conversion of the nitration reaction*

Temperature (°C)	Conversion rate (%)
25	94.6
30	92.7
40	97.0
50	89.2

180

181 Table 4 shows that the reaction conversion rate (the production of all molecules A, B and C)  
182 varies with temperature and is maximal at 40 °C. The selectivity of B and C was determined  
183 by using the iodine index method.

#### 184 3.3.2 Determination of the molecules selectivity

185 The iodine number of oils and fats measures their unsaturation degree. The Wijs method [20],  
186 commonly used, requires 30 min absorption time. Sodium thiosulfate solution 0.1M was used  
187 as a titration reactant. The measurement of the biodiesel iodine index before and after the  
188 nitration reaction allowed to calculate the conversion of unsaturations (the loss of the double  
189 bonds). This value was used to determine the proportion of molecules B and C according to  
190 the equation 3-1.

191 
$$X = \frac{\text{iodine index } t_0 - \text{iodine index } t_f}{\text{iodine index } t_0} \quad 3-1$$

192 The proportion of A was obtained by making a difference between the conversion rate of the  
 193 reaction (Table 4) and the unsaturations conversion rate. Results are gathered in Table 5  
 194 which shows that at high synthesis temperature, the selectivity of B and C decreases.

195 *Table 5: Determination of the molecule's selectivity*

Temperature °C	Total conversion rate (%)	Selectivity of B and C (%)	Selectivity of A (%)
25	94.6	95.2	4.8
30	92.7	68.0	32.0
40	97.0	42.9	57.1
50	89.2	41.6	58.4

196  
 197 The results obtained in this study show that the reaction mechanism of biodiesel nitration  
 198 (aliphatic chain) is more complex than that of the aromatic compounds. Indeed, three  
 199 molecules with different selectivity had been identified (Table 5).

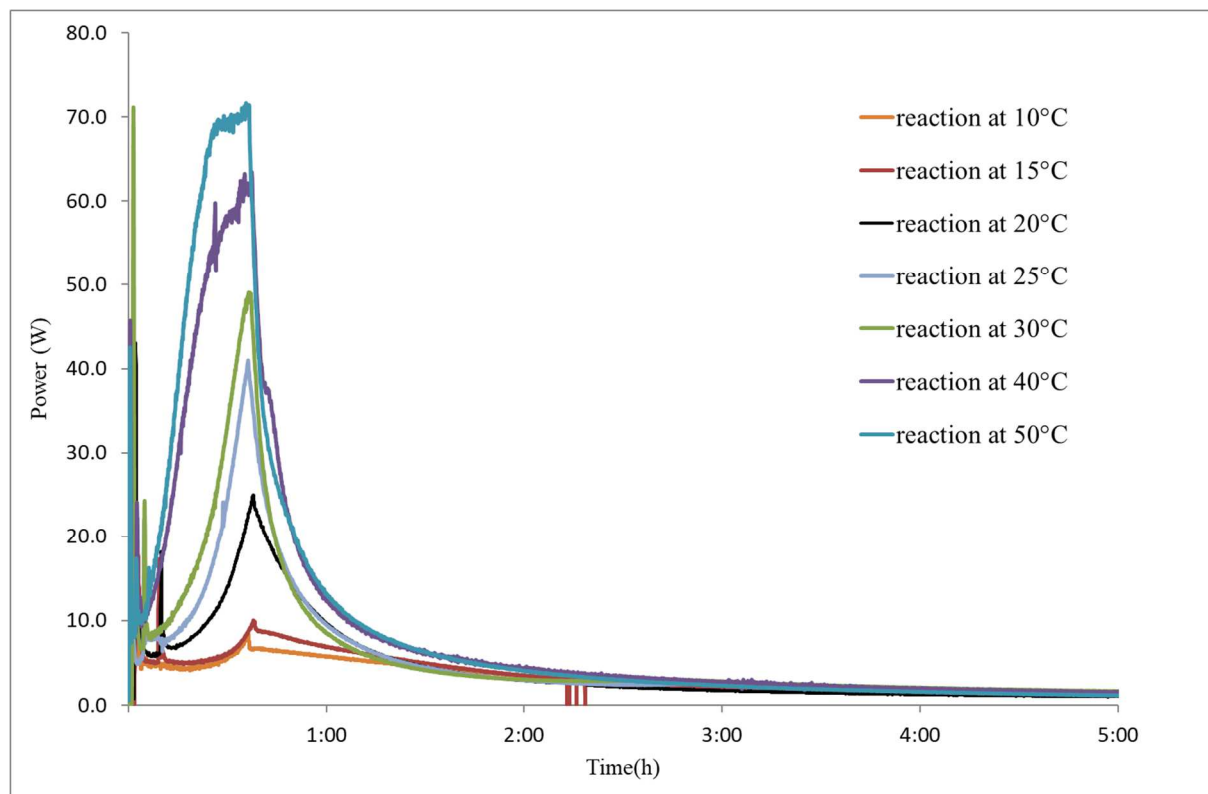
200 During the synthesis at low temperature (below 20°C), the final product is a stable micro  
 201 emulsion preventing phase separation. This stability may be due to the hydrophilic behavior  
 202 of the saturated nitrated products (B and C) at low temperatures.

## 203 4 Calorimetric study

### 204 4.1 Determination of the reaction heat

205 The integration of the experimental power profiles (equation 4-1) obtained according to the  
 206 conditions presented in section 3, shows that the heat released by the reaction varies with the  
 207 temperature (Table 6). This change in the thermal behavior has also been observed by Chen et  
 208 *al* 2012 [21] in their work about the nitration of iso-octanol but no interpretation has been  
 209 given. Power profiles ( $q_r$ ) are shown in Fig.5. Sudden variation of the thermal power with  
 210 time at the beginning of the reaction corresponds to the nitration of the small amount of the  
 211 products as Methyl linolenate and Methyl linoleate. Such thermal behavior may present a risk  
 212 of thermal runaway.

213 
$$Q_R^{\text{Exp}} = \int_{t_0}^t q_r dt \quad 4-1$$



215

216

Fig.5. Power profiles at different temperatures

217

Table 6: Heat released by the synthesis reaction at different temperatures

Temperature °C	Heat (kJ)	Conversion rate (%)
25	112.5	94.6
30	106.3	92.8
40	161.9	97.0
50	171.9	89.2

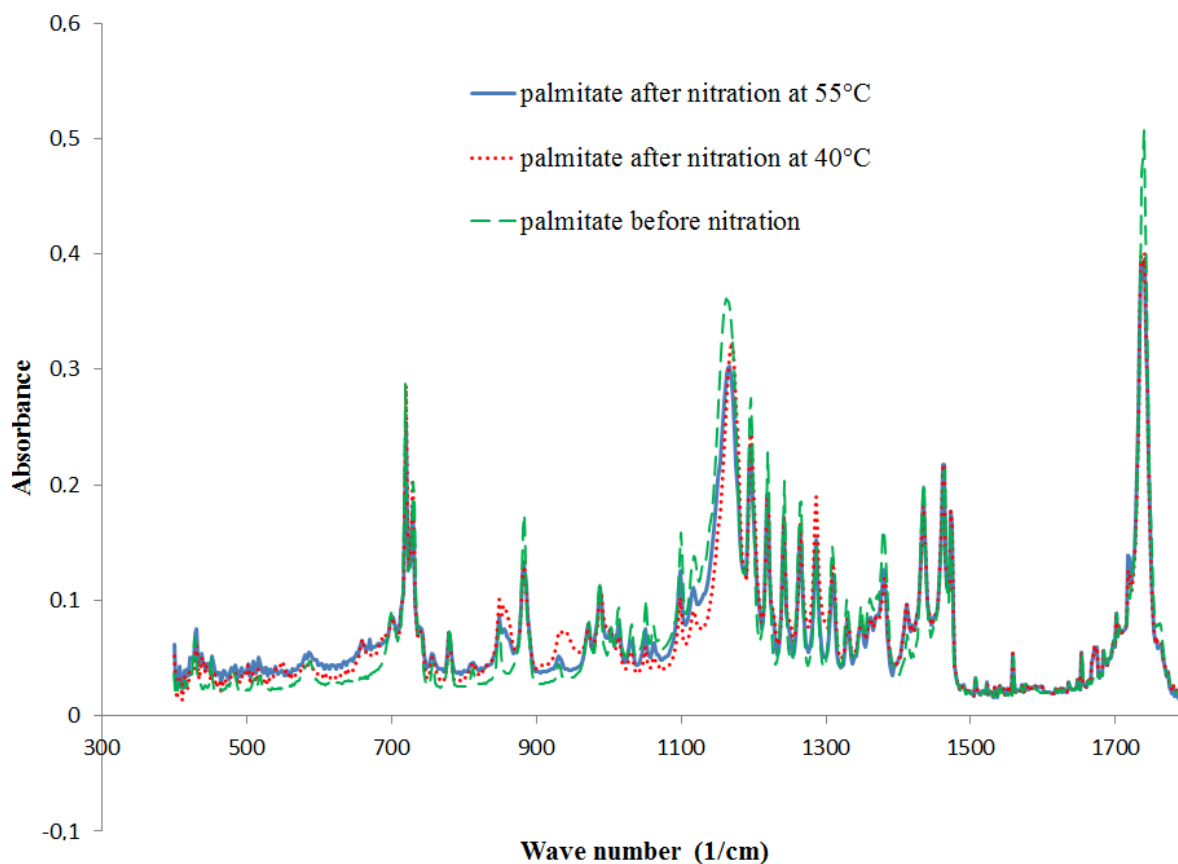
218 The total heat released by the reaction (table 6) represents all the thermal effects linked to the  
 219 products synthesis, to the mixing phenomena and to the possible decomposition in case of  
 220 unstable compound. In section 3.3.2, a modification of the reaction mechanism according to  
 221 the synthesis temperature was noticed. In addition to other phenomena mentioned above, the  
 222 modification of the reaction mechanism is likely to contribute to the change in the total heat  
 223 released by the reaction.

224 Heat related to the mixing phenomena and the decomposition of unstable compounds are  
 225 presented in sections 4.2 and 4.3.

## 226 4.2 Heat of mixing measurement

227 To measure the heat of mixing, the power profile obtained without nitration reaction have to  
 228 be integrated. The operating conditions were kept identical to those in the synthesis reaction  
 229 (section 3.1) except for the biodiesel reactant. In fact, to avoid the nitration reaction, the  
 230 biodiesel was replaced by a molecule close to its main molecule (methyl oleate): methyl  
 231 palmitate.

232 The absence of the reaction was confirmed by the palmitate infrared spectrum after the  
233 reaction (fig.6: no nitro group was detected). The non-reactivity of the methyl palmitate is due  
234 to the absence of unsaturated carbons.

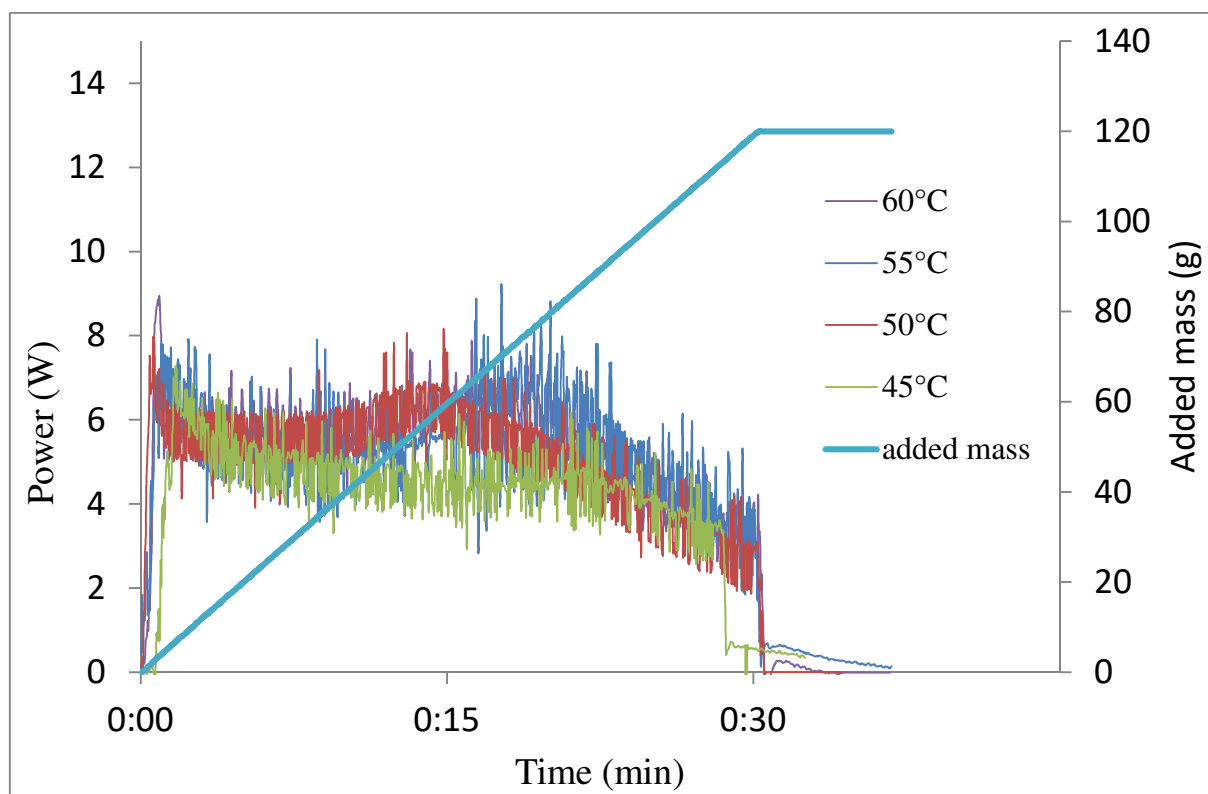


235

236

Fig. 6: Methyl palmitate IR spectrum before and after the reaction

237 The heat of mixing below 40°C could not be measured because the melting point of methyl  
238 palmitate is higher than 35°C.



239

240

Fig.7. Power profiles obtained with the palmitate

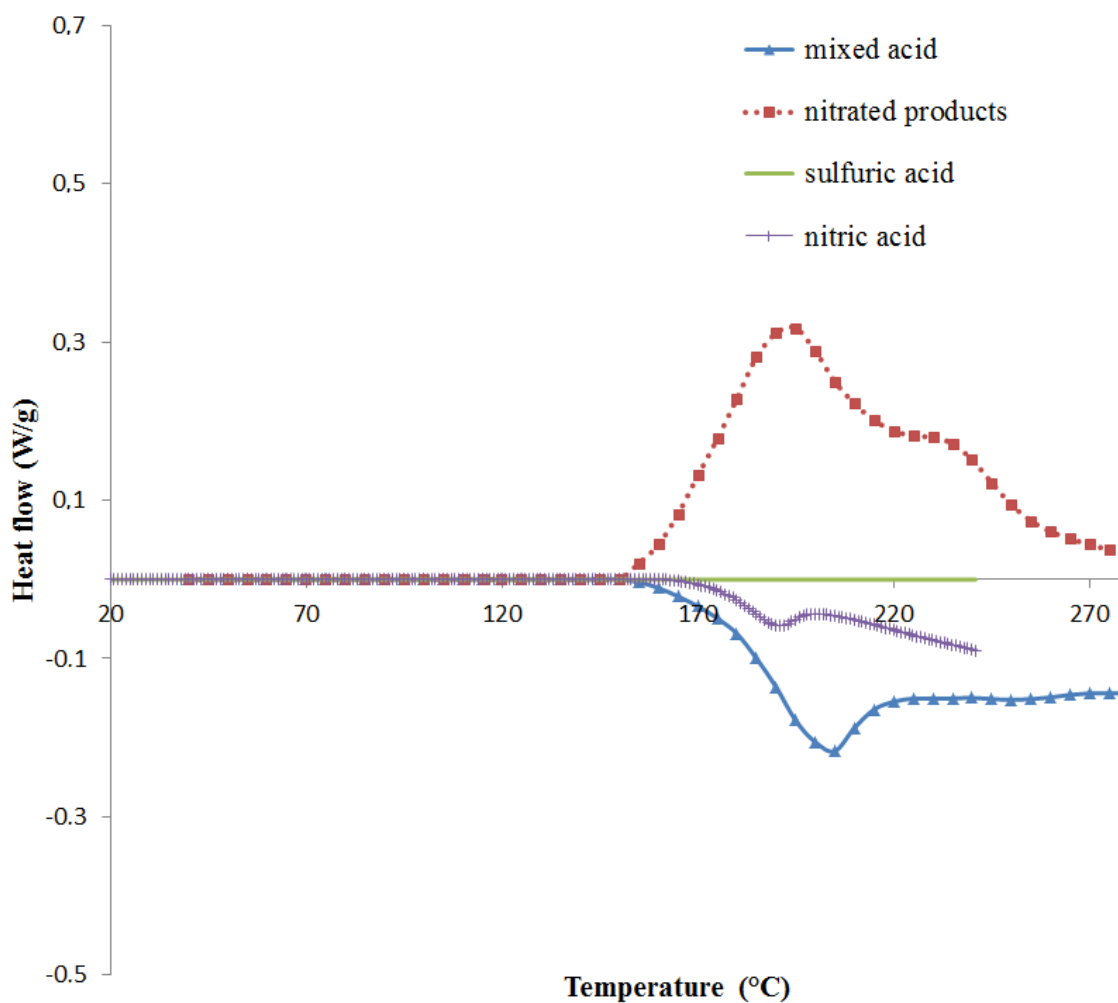
241 Fig.7. shows that the power profiles are identical regardless of the temperature. The average  
 242 heat is about 8J. All power profiles return to the baseline at the end of the addition,  
 243 demonstrating the absence of any chemical transformations.

#### 244 4.3 Measurement of the decomposition heat

245 The measurement of the heat released during the decomposition was done in two steps. Pure  
 246 products: nitrated products, nitric acid, sulfuric acid and mixed acid (sulfo-nitric acid) were  
 247 analyzed first (fig.8), then samples of mixed acid with different percentages (w/w) of nitrated  
 248 products (fig.9). These analyses were realized using a DSC in a non-isothermal mode with  
 249 Gold-plated high-pressure crucibles and a heating rate of  $2^{\circ}\text{C}\cdot\text{min}^{-1}$ . According to Liu et al  
 250 [22], the advantage of DSC test under non-isothermal condition is its swiftness and high  
 251 efficiency in a short time.

252 For pure products (fig.8) no signal of decomposition is observed in our range of synthesis  
 253 temperature ( $<50^{\circ}\text{C}$ ). The only thermal effects are detected beyond synthesis temperatures.  
 254 Nitric acid and mixed acid's DSC curves show an endothermic effect at  $T_{onset} = 181.3^{\circ}\text{C}$   
 255 which is attributed to the decomposition of the nitric acid [23]. This temperature was  
 256 determined by the tangent method from zero curvature. Regarding to the nitrated product, it  
 257 exhibits an exothermic peak at  $T_{onset} = 150.9^{\circ}\text{C}$  which correspond to its decomposition. Its  
 258 thermal instability was mentioned in other works [9] [24] [21]. The  $T_{onset}$  of our additive  
 259 decomposition is closed to that of fossil nitrated product (EHN) [8].

260

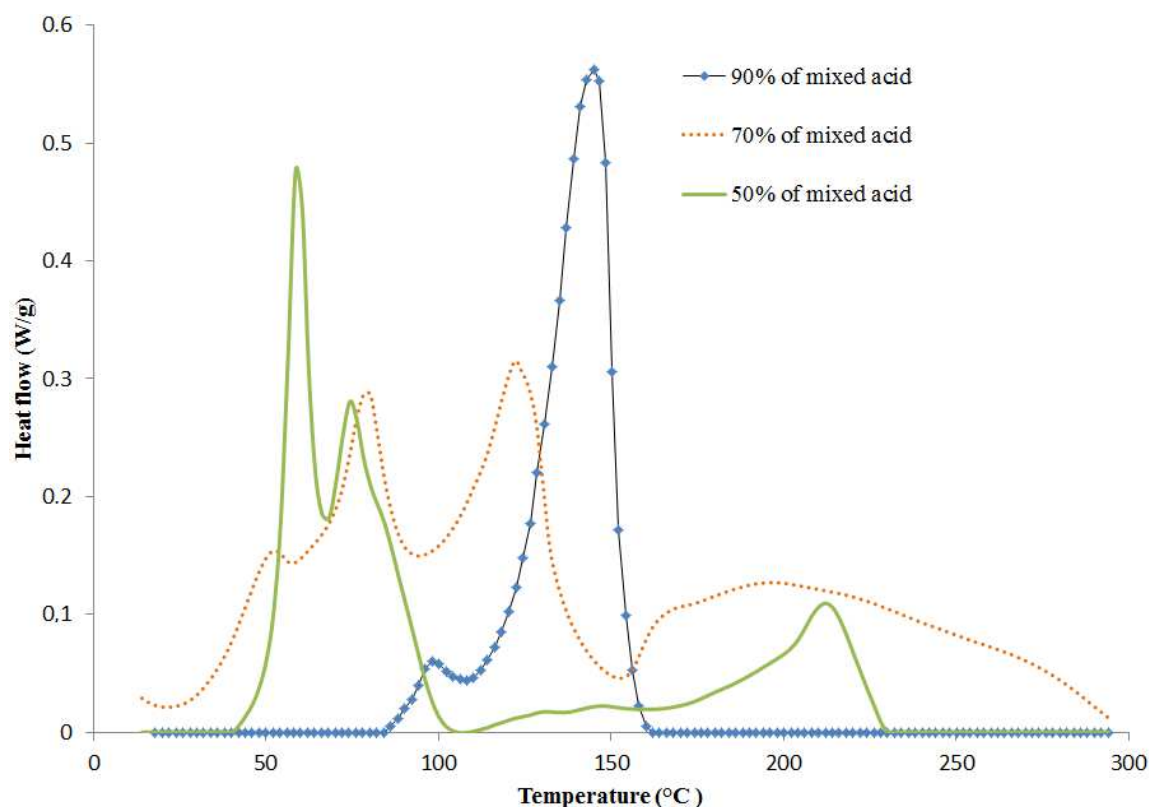


262

263

Fig. 8. Pure sulfo-nitric acid and pure nitrated product decomposition

264 Fig.9 shows the DSC curves of sulfo-nitric acid mixed with nitrated products. The initial  
 265 decomposition temperatures  $T_{onset}$  are 48.83°C, 70.39°C and 77.96°C respectively for 50 %,  
 266 70% and 90% of mixed acid. Obviously, when the quantity of nitrated products added into the  
 267 mixed acid increased, lower onset temperatures are observed. It is also noted that the specific  
 268 enthalpy decreases with the amount of nitrated products (table 7). This enthalpy ( $\Delta H$ ) reported  
 269 to the total sample mass was determined by integrating the area under the exothermic curve.



270

271

Fig.9. Study of the decomposition mixed sulfo-nitric and nitrated products

272 This study allows to demonstrate that the decomposition of the sulfo-nitric mixed acid and  
 273 nitrated products also contributes to the modification of the total heat released during the  
 274 synthesis reaction (Fig.5).

275

Table 7: Results of DSC analysis

Component of sample (w/w)	$T_{onset}$ (°C)	$\Delta H$ (J/g)
90% of mixed acid and 10% nitrated products	77.96	502.0
70% of mixed acid 30% nitrated products	70.39	474.1
50% of mixed acid 50% nitrated products	48.83	332.1

276

#### 277 4.4 Study of the safety parameters

278 In the light of the strong exothermicity of the nitration reaction and the mixed acid  
 279 decomposition in the presence of the nitrated products, the determination of the Maximum  
 280 Temperature of the Synthesis Reaction (*MTSR*) is more than necessary to avoid the possible  
 281 risk of thermal runaway.

282 The Maximum Temperature of Synthesis Reaction (*MSTR*) is the temperature reached by the  
 283 reaction mixture if the energy potential of the main reactions is released under adiabatic  
 284 conditions [25].

285 This decomposition releases an excess of energy causing a thermal runaway. To evaluate this  
 286 temperature, it is necessary to determine the  $\Delta T_{ad}$  (the temperature variation in adiabatic  
 287 mode) according to equation 4-2.

$$288 \quad \Delta T_{ad} = \frac{Q_R^{exp}}{C_p M_r X'_r} \quad 4-2$$

289 with  $C_p$  the heat capacity of reaction mixture obtained with reaction calorimeter,  $M_r$  the mass  
 290 of the reaction mixture and  $X'_r$  the full conversion of the biodiesel.

291 The calculation of the  $MTSR$  was done in semi-batch mode according to equation 4-3 [26]  
 292 [25]. The results are given in Table 8. They show a considerable increase in  $MTSR$  from an  
 293 isothermal of 40 °C. This can be explained by the fact that the value of the adiabatic  
 294 temperature increase  $\Delta T_{ad}$  used for the calculation of  $MTSR$ , considers the enthalpy of the  
 295 nitration reaction in addition to the decomposition enthalpy.

$$296 \quad MTSR = T_P + \Delta T_{ad} \cdot X_{ac, max} \quad 4-3$$

297 with  $X_{ac, max}$  the maximum accumulation of the unreacted reactant and  $T_P$  the synthesis  
 298 temperature.

299 In our case, the nitric acid is in stoichiometric excess over biodiesel. Thus  $X_{ac, max}$  is obtained  
 300 at the end of the addition.

301 Table 8: Safety parameters of nitration reaction

Temperature (°C)	Conversion (%)	$C_p$ (J·g <sup>-1</sup> ·°C <sup>-1</sup> )	$\Delta T_{ad}$ (°C)	$X_{ac, max}$ (%)	$MTSR$ (°C)
25	94.6	2.1	194.4	30.3	83.8
30	92.8	2.0	194.8	36.5	101.2
40	97.0	2.2	262.8	49.5	171.1
50	89.2	2.1	313.6	50.5	208.5

302 If we compare results in table 7 with those in table 8, it appears that the lowest  $MTSR$   
 303 (83.8°C) is higher than the maximum  $T_{onset}$  obtained in decomposition study (77.96°C). In  
 304 case of loss of temperature control, this means that the decomposition reaction would be  
 305 triggered before completion of the synthesis reaction, which would further lead to very severe  
 306 consequences. According to Stoessel's criticality index used for the risk assessment of a  
 307 chemical reaction [27], this implies that the runaway is too fast for a safety barrier to be  
 308 efficient. These results correspond to a Stoessel's criticality class of 5 if the nitration reaction  
 309 conducted in these operated conditions.



## 310 5 Measurement of the bio-additive cetane number (index)

311 The cetane number is the measurement of the diesel fuel ignition performance. It is obtained  
312 by making some comparison with reference fuels in a standardized test. Higher cetane number  
313 indicates that the ignition properties of the fuel are better [28]. This index is obtained  
314 according to ASTM D 613. The equipment used was a Cooperative Fuel Research (CFR)  
315 engine. A standard diesel of cetane number 50 was used to prepare two samples of 1% and  
316 5% concentration in bio-additive. For each mixture, the cetane number was measured at two  
317 synthesis temperatures 25 and 40 °C. The results of the cetane number analysis are listed in  
318 Table 9. They show that the bio-additive synthesized in this study allows to increase the  
319 cetane number of the reference diesel. A 5% addition of the bio-additive to the reference  
320 diesel improves the cetane number by 3 points.

321 Table 9: Cetane number with the CFR engine

Synthesis temperature (°C)	CN fuel		
	CN fuel	CN fuel +1% additive	+ 5% additive
25	50.0	50.9	52.9
40	50.0	50.9	53.2

322 Canoira *et al* 2012 [13] obtained a 5 points increase in the fuel cetane number by mixing their  
323 nitrated biodiesel to fossil diesel in a concentration of 1000 mg.L<sup>-1</sup>. With our bio-additive a  
324 5% addition (concentration of 49g.L<sup>-1</sup>) to the reference diesel improves the cetane number by  
325 3 points. It seems clear that our bio-additive is much less efficient than Canoira *et al* one. It  
326 may be due to the fact that Canoira *et al* used a biodiesel containing 33.0 %, 54.20% and 16%  
327 of methyl linoleate while ours contains only 2.5%. According to Abdullah *et al* 2010 [16],  
328 during the nitration process of biodiesel, NO<sub>3</sub> or NO<sub>2</sub> groups are grafted to the double bonds  
329 of carbon atoms. Based on this statement, biodiesel containing more double bonds, once  
330 nitrated, tend to be more energetic than others. That could explain the big different between  
331 these 2 results.

332 However, the difference between our additive and the EHN is not so high. Indeed a 2.5% and  
333 a 5% addition of EHN on BN20 (diesel with 20% of methyl ester) leads respectively to an  
334 increase in cetane number of 2.5 and 6.5 points [29].

## 335 6 Conclusion

336 The results of chemical analysis of the nitrated products showed the presence of 3 different  
337 compounds (methyl-8-nitro oleate, methyl-10-nitrate stearate and methyl-10-nitrate-9-  
338 nitrostearate), whose selectivity varies according to the synthesis temperature. Some of these  
339 compounds, particularly the methyl-8-nitro oleate and the methyl-10-nitrate-9-nitrostearate,  
340 were also identified by Canoira *et al.* [13] and Malins *et al.* [30].

341 The heat released by the chemical transformation obtained with the reaction calorimeter RC1-  
342 *RTCal* varies with the synthesis temperature. This difference in the thermal behavior is due to  
343 the complexity of the reaction mechanism as well as the instability of the nitrated products  
344 and sulfo-nitric acid mixture. The study of the thermal stability shows that the  $T_{onset}$  of the  
345 decomposition is around 40°C. Thus, at high synthesis temperature (beyond the  $T_{onset}$ ), the  
346 heat measured by the RC1 corresponds to the sum of the heat released by the nitration  
347 reaction and that of the mixture decomposition. This thermal and chemical behavior shows  
348 the complexity of the aliphatic compound nitration compared to the aromatic compounds one.

349 The modification of thermal behavior according to the synthesis temperature increases the  
350 risk of thermal runaway. The Maximum Temperature of the Synthesis Reaction (*MTSR*)  
351 obtained is higher than the sulfo-nitric acid temperature of decomposition, which leads to  
352 important risks of thermal runaway. To avoid thermal runaway while having a high conversion  
353 rate, the synthesis temperature, the flow rate of sulfo-nitric acid as well as the temperature  
354 control of the cooling fluid are the main parameters on which we can lean on.

### 355 **Acknowledgments**

356 The authors thank AMED project. The AMED project has been funded with the support  
357 of the European Union with the European Regional Development Fund (ERDF) and the  
358 Regional Council of Normandy.

359 The authors particularly thank Arnaud BARBIER for his help on chemical analyses.

### 360 **References**

- 361 [1] World Energy Outlook 2017. IEA Webstore n.d. [https://webstore.iea.org/world-energy-](https://webstore.iea.org/world-energy-outlook-2017)  
362 [outlook-2017](https://webstore.iea.org/world-energy-outlook-2017) (accessed July 12, 2018).
- 363 [2] Courtils ND, Durand D, Mabilon G, Prigent M. La dépollution des gaz d'échappement  
364 diesel au moyen de pots catalytiques d'oxydation. *Sci Total Environ* 1993;134:295–304.  
365 doi:10.1016/0048-9697(93)90359-E.
- 366 [3] Song C. *Chemistry of Diesel Fuels*. CRC Press; 2000.
- 367 [4] Beatrice C, Bertoli C, Giacomo ND. *The Influence of Fuel Formulations on Pollutant of*  
368 *a Light Duty D.I. Diesel Engine*. Warrendale, PA: SAE International; 1996.  
369 doi:10.4271/961972.
- 370 [5] Suppes GJ, Rui Y, Rome AC, Chen Z. Cetane-Improver Analysis and Impact of  
371 Activation Energy on the Relative Performance of 2-Ethylhexyl Nitrate and  
372 Tetraethylene Glycol Dinitrate. *Ind Eng Chem Res* 1997;36:4397–404.  
373 doi:10.1021/ie9702284.
- 374 [6] Velmurugan K, Gowtham S. Effect of cetane improver additives on emissions. *Int J*  
375 *Mod Eng Res* 2012;2:3372–3375.
- 376 [7] Quadros PA, Oliveira NMC, Baptista CMSG. Benzene nitration: validation of  
377 heterogeneous reaction models. *Chem Eng Sci* 2004;59:5449–54.  
378 doi:10.1016/j.ces.2004.07.107.
- 379 [8] Chen L-P, Liu T-T, Yang Q, Chen W-H. Thermal hazard evaluation for iso-octanol  
380 nitration with mixed acid. *J Loss Prev Process Ind* 2012;25:631–5.  
381 doi:10.1016/j.jlp.2012.01.008.
- 382 [9] Ting Yang, Liping Chen, Wanghua Chen. Thermal stability of 2-ethylhexyl nitrate with  
383 acid. ResearchGate n.d.  
384 [https://www.researchgate.net/publication/271659120\\_Thermal\\_stability\\_of\\_2-](https://www.researchgate.net/publication/271659120_Thermal_stability_of_2-ethylhexyl_nitrate_with_acid)  
385 [ethylhexyl\\_nitrate\\_with\\_acid](https://www.researchgate.net/publication/271659120_Thermal_stability_of_2-ethylhexyl_nitrate_with_acid) (accessed June 19, 2018).

- 386 [10] Wang K, Liu D, Xu S, Cai G. Research on the thermal history's influence on the thermal  
387 stability of EHN and NC. *Thermochim Acta* 2015;610:23–8.  
388 doi:10.1016/j.tca.2015.04.022.
- 389 [11] Schmidt CW. BIODIESEL Cultivating Alternative Fuels. *Environ Health Perspect*  
390 2007;115:A86–91.
- 391 [12] Johnson DM, Edgar DW, Edgar LD, Pate M, Steffen RW. Biodiesel: Awareness, Use  
392 and Perceptions of Students at Four U. S. Universities. *NACTA J* 2015;59:54–62.
- 393 [13] Canoira L, Alcántara R, Torcal S, Tsiouvaras N, Lois E, Korres DM. Nitration of  
394 biodiesel of waste oil: Nitrated biodiesel as a cetane number enhancer. *Fuel*  
395 2007;86:965–71. doi:10.1016/j.fuel.2006.10.022.
- 396 [14] Madden MC. Comparative toxicity and mutagenicity of soy-biodiesel and petroleum-  
397 diesel emissions: overview of studies from the U.S. EPA, Research Triangle Park, NC.  
398 *Inhal Toxicol* 2015;27:511–4. doi:10.3109/08958378.2015.1107153.
- 399 [15] Riadi L, Widiyanto AY, Purwanto E, Pono A, Theresia R. Synthesis of biodiesel from  
400 waste cooking oil by two steps process transesterification and ozonation 2015.
- 401 [16] Abdullah A, Wicakso DR, Junaidi AB, Badruzaufari B. PRODUCTION OF CETANE  
402 IMPROVER FROM *Jathropa curcas* OIL. *Indones J Chem* 2010;10:396–400.
- 403 [17] A. V. Topchiev. Nitration of Hydrocarbons and Other Organic Compounds - 1st Edition  
404 1959. [https://www.elsevier.com/books/nitration-of-hydrocarbons-and-other-organic-](https://www.elsevier.com/books/nitration-of-hydrocarbons-and-other-organic-compounds/topchiev/978-0-08-009154-9)  
405 [compounds/topchiev/978-0-08-009154-9](https://www.elsevier.com/books/nitration-of-hydrocarbons-and-other-organic-compounds/topchiev/978-0-08-009154-9) (accessed September 14, 2018).
- 406 [18] Ben Talouba I, Balland L, Mouhab N, Bensahla N. Kinetic and safety parameters of  
407 decomposition of neat Tert-Butyl (2-Ethylhexyl) monoperoxy Carbonate and in organic  
408 solvents. *Thermochim Acta* 2018;659:105–12. doi:10.1016/j.tca.2017.09.022.
- 409 [19] Shimkin A. Optimization of DSC calibration procedure. *Thermochim Acta*  
410 2013;566:71–6. doi:10.1016/j.tca.2013.04.039.
- 411 [20] Sahoré AD, Abouattier JL. Quelques méthodes d'analyse biochimique de produits  
412 alimentaires. Editions Publibook; 2016.
- 413 [21] Chen L-P, Liu T-T, Yang Q, Chen W-H. Thermal hazard evaluation for iso-octanol  
414 nitration with mixed acid. *J Loss Prev Process Ind* 2012;25:631–5.  
415 doi:10.1016/j.jlp.2012.01.008.
- 416 [22] Liu SH, Hou HY, Chen JW, Weng SY, Lin YC, Shu CM. Effects of thermal runaway  
417 hazard for three organic peroxides conducted by acids and alkalines with DSC, VSP2,  
418 and TAM III. *Thermochim Acta* 2013;566:226–32. doi:10.1016/j.tca.2013.05.029.
- 419 [23] Kazakov AI, Rubtsov YI, Andrienko LP, Manelis GB. Kinetics and mechanism of  
420 thermal decomposition of nitric acid in sulfuric acid solutions. *Russ Chem Bull*  
421 1987;36:1999–2002.
- 422 [24] Zeng X, Chen W, Liu J. Molecular Structure, Electronic Structure and Heats of  
423 Formation of Explosive Sensitizers. *Acta Phys-Chim Sin* 2007;23:192–7.  
424 doi:10.1016/S1872-1508(07)60015-1.
- 425 [25] Lerena P, Wehner W, Weber H, Stoessel F. Assessment of hazards linked to  
426 accumulation in semi-batch reactors. *Thermochim Acta* 1996;289:127–42.  
427 doi:10.1016/S0040-6031(96)03024-9.
- 428 [26] Zichao G, lerena, Peng Z, Liping C. Insights into maximum temperature of synthesis  
429 reactions in isothermal homogeneous semibatch reactors 2018.  
430 doi:10.1016/j.tca.2018.08.018.
- 431 [27] Stoessel F. Planning protection measures against runaway reactions using criticality  
432 classes. *Process Saf Environ Prot* 2009;87:105–12. doi:10.1016/j.psep.2008.08.003.
- 433 [28] Li R, Wang Z, Ni P, Zhao Y, Li M, Li L. Effects of cetane number improvers on the  
434 performance of diesel engine fuelled with methanol/biodiesel blend. *Fuel* 2014;128:180–  
435 7. doi:10.1016/j.fuel.2014.03.011.

- 436 [29] R. Sathiyamoorthi, S. Chezian Babu, V. Rajangam, L. S. Tamizhselvan, Panimalar  
437 Engineering College, poonamallee, chennai, Tamil Nadu. Evaluation of Neem oil  
438 biodiesel with 2-Ethyl Hexyl Nitrate 2-EHN as Cetane Improver on Performance and  
439 Emission characteristics of a DI Diesel Engine. Int J Eng Res 2018;V6.  
440 doi:10.17577/IJERTCON071.
- 441 [30] Malins DC, Houle CR. Nitration of methyl oleate with acetyl nitrate: a synthesis of  
442 methyl aminostearate. J Am Oil Chem Soc 1963;40:43–45.  
443